VARIATION OF CPTU PARAMETERS AND LIQUEFACTION POTENTIAL AT A RECLAIMED LAND INDUCED BY DYNAMIC COMPACTION

Chih-Sheng Ku [1] and C. Hsein Juang [2]

ABSTRACT

This paper presents results of an extensive field investigation of a hydraulic-filled site with cone penetration testing before and after ground improvement by dynamic compaction. The focus of the paper is to examine the effect of dynamic compaction on the cone penetration sounding characteristics and liquefaction hazards at the site. The results show that cone penetration testing is an effective tool for investigating the effect of dynamic compaction. The results also show that while significant changes in CPTu parameters are observed after the dynamic compaction, the soil behavior type determined with these CPTu parameters largely remains unchanged. Furthermore, in terms of the two measures of liquefaction hazards, the liquefaction potential index and the liquefaction-induced settlement, the risk is significantly reduced by the dynamic compaction.

Key words: Cone penetration testing, dynamic compaction, reclaimed land, liquefaction.

1. INTRODUCTION

The reclaimed lands and artificial islands are generally created by hydraulic filling of the dredged material, mostly consisting of loose silty fines sands. Coupling with high groundwater table and active seismicity, these lands generally have a high potential for liquefaction. To mitigate possible liquefaction hazards, it is essential to densify the reclaimed lands. For ground improvement over a large area, dynamic compaction (Leonards *et al*. 1980; Mayne *et al*. 1984; Pan and Hwang 1995; Chang *et al*. 2002; Rollins and Kim 2010) is often employed. The process primarily consists of dropping a heavy weight repeatedly on the ground at regular intervals. The stress waves generated by the hammer (or tamper) drops typically can densify the ground within a depth of approximately 10 m. The effectiveness of dynamic compaction for ground densification depends on several factors, such as the type of soils, the depth to the groundwater table, and the tamping pattern and parameters (grid dimensions, number of passes, weight of tamper, height of drop, number of drops, *etc*.). In many cases, trial tamping program may be needed.

Use of dynamic compaction to mitigate liquefaction hazards has been reported (Lee *et al*. 2001; Majdi *et al*. 2009). In practice, in situ testing such as standard penetration test (SPT) or cone penetration test (CPT) is often employed to investigate the site before and after dynamic compaction. CPT is particularly suitable for such investigation because of its capability of continuous profiling and superiority in obtaining repeatable measurement over other in situ tests. In fact, it has become the most commonly used technique for quality control of field compaction projects (Pan and Hwang 1995; Massarsch and Fellenius 2002).

Manuscript received March 24, 2011; revised June 20, 2011; accepted June 22, 2011.

[1] Associate Professor (corresponding author), Department of Civil and Ecological Engineering, I-Shou University, Kaohsiung 840, Taiwan (e-mail: csku@isu.edu.tw).

[2] Professor, Department of Civil Engineering, Clemson University, Clemson, South Carolina 29634, U.S.A.

In this paper, a case study of the effect of dynamic compaction at a reclaimed land for mitigation of liquefaction hazards is presented. Numerous piezocone penetration (CPTu) soundings are conducted before and after dynamic compaction. The emphasis of the paper is placed on the examination of the cone penetration sounding characteristics and liquefaction hazards at the site before and after dynamic compaction. Results of the detailed examination are presented and discussed.

2. SITE LOCATION AND GEOLOGICAL CONDITIONS

Taichung Harbor, a man-made harbor, is located on the coastal plain between Tachia and Tatu rivers, approximately in the middle of the west coast of Taiwan (Fig. 1(a)). The Harbor occupies an area with a length of approximately 12.5 km in the north-south direction and a width ranging from 2.5 km to 4.5 km in the east-west direction (Fig. 1(b)). The study site is located in the Port (Fig 1(c)), which is designated for crude oil-related chemical industrial park.

The surficial soils in the Harbor area are basically alluvial deposits from Tachia and Tatu rivers. The thick alluvium, which was the deposit from the two rivers under the interaction of tide, wave, and wind, covers the coastal plain. These alluvial deposits are composed of alternating silty-sand, sandy-silt, clayey-silt, and silty-clay. The geologic structure of special interest here is the Chinshui Fault, an active fault roughly 6 km away from the site.

The study site is a reclaimed land that was created by hydraulic filling. Field investigations show that the groundwater table is located at approximately 3.0 m to 3.8 m below the ground surface. The layout of bored holes and cone penetration (CPT) soundings before the ground improvement work at the site is depicted in Fig. 2. Based on bored holes information and CPT soundings, the subsurface soil profiles are depicted with Figs. 3 and 4, respectively, for cross-sections AB and CD (Fig. 2). Basically, the subsurface at the site consists of the following layers:

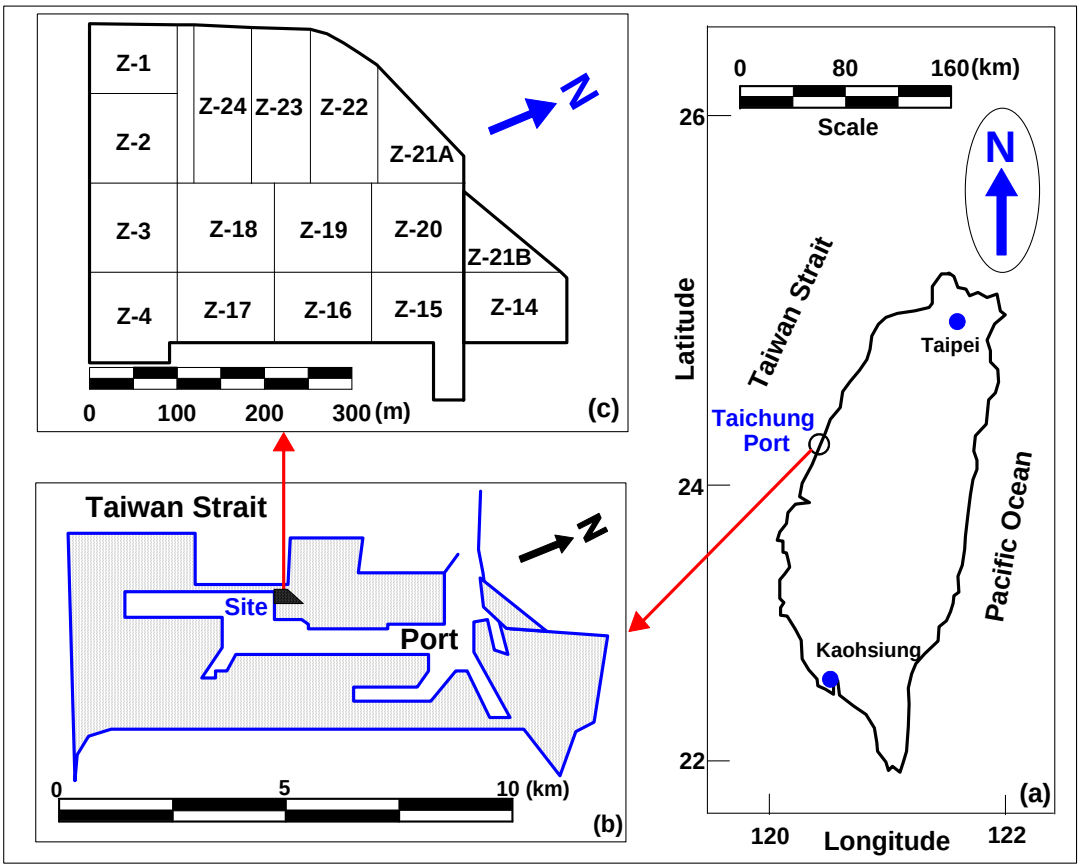

Fig. 1 Location of the study site

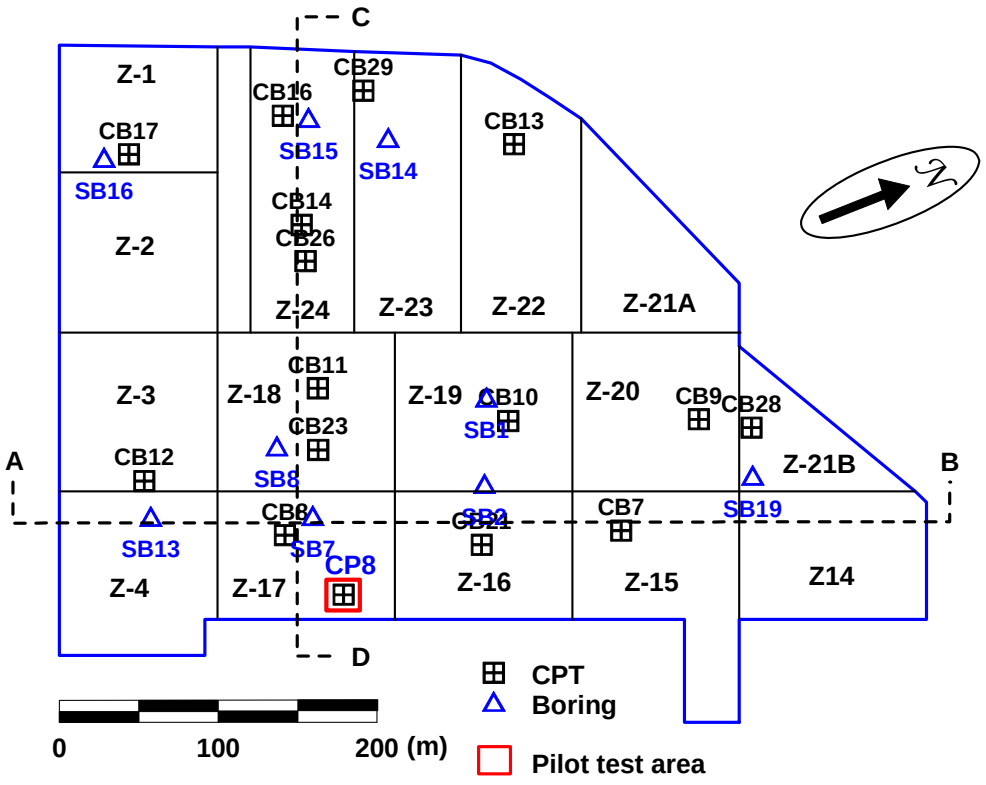

Fig. 2 Layout of field tests before the ground improvement work at the site

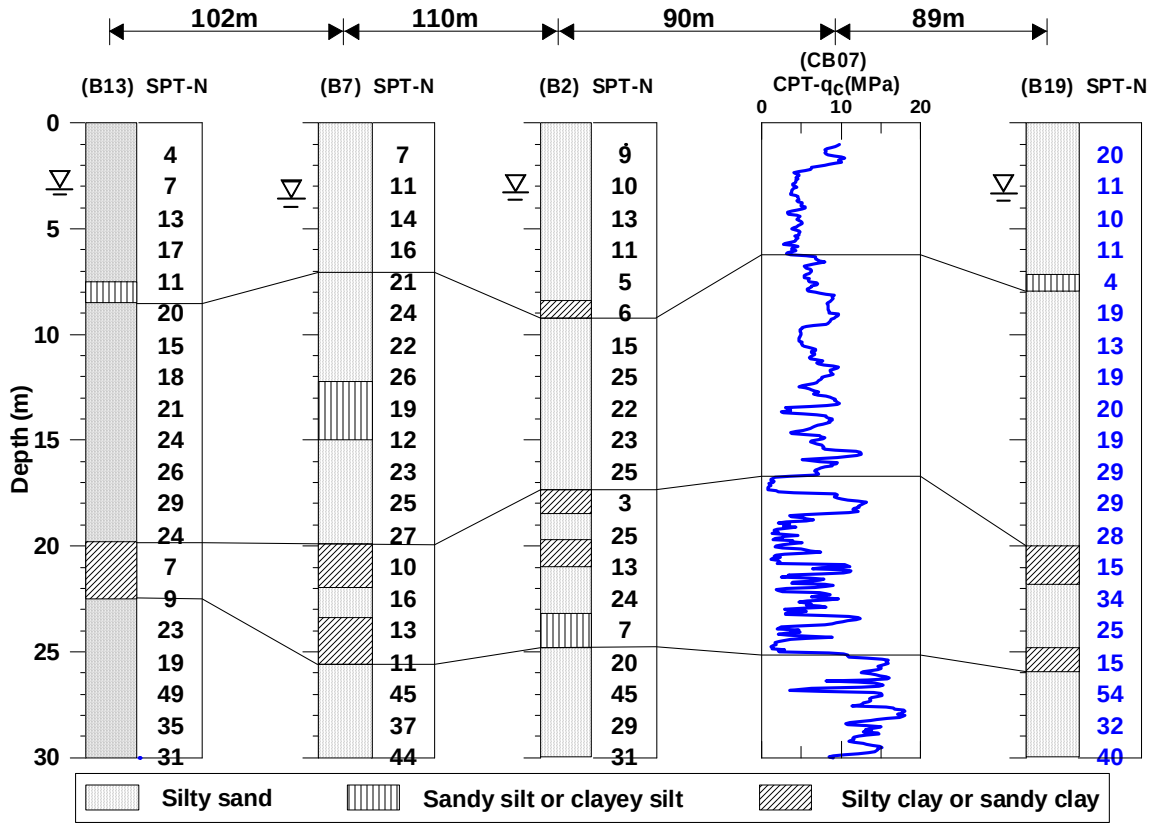

Fig. 3 Soil profile along the A-B section at the site

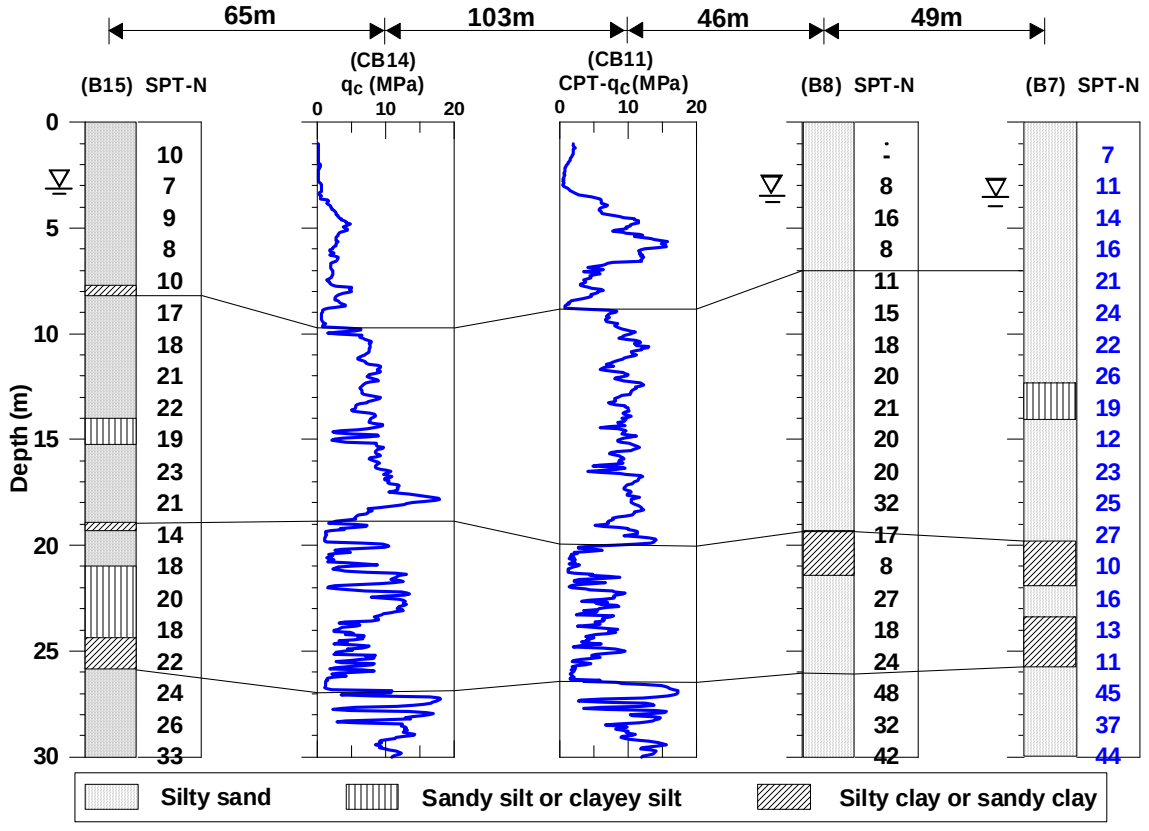

Fig. 4 Soil profile along the C-D section at the site

1. *Silty fine sand layer*: Roughly from the ground surface to a depth of 8 m. It mainly consists of gray silty fine sand, with trace of silty clay and sandy silt. The standard penetration blow counts are generally in the range of 4 to 20, with an average of approximately 10. The unit weight of the soil is equal to 18.3 kN/m^3 and the natural water content ranges from 22.4% to 26.2%. This layer is best characterized as loose sand.
2. *Silty sand or sandy silt*: Roughly between the depths 8 m and 20 m. This layer mainly consists of gray silty fine to medium sand, with layers of sandy silt. The standard penetration blow counts are generally in the range of 12 to 32, with an average of 21. The unit weight of the soil is equal to 19.1 kN/m^3 and the natural water content ranges from 24.7% to 27.6%. This layer is best characterized as medium dense sand.
3. *Silty clay and silt*: Roughly between the depths of 20 m and 26 m. This layer mainly consists of gray silty clay with fine sand and sandy silt. The standard penetration blow counts are generally in the range of 7 to 15. The unit weight of the soil is equal to 18.4 kN/m^3 and the natural water content ranges from 23% to 30%. The liquid limits are in the range of 24% to 33%, and the plasticity index ranges from 5 to 11. This layer is best characterized as medium stiff to stiff clay.
4. *Silty fine sand*: Roughly between the depths of 26 m and 30 m. The standard penetration blow counts are generally in the range of 24 to 54, with an average of 38. The unit weight of the soil is equal to 20.0 kN/m^3 and the natural water content ranges from 19% to 25%. This layer is best characterized as dense sand.

3. DYNAMIC COMPACTION WORK

The site was considered susceptible to liquefaction and ground improvement was deemed necessary (Yu *et al*. 2000). Dynamic compaction was selected for ground improvement. The site was divided into 15 zones, each with an area of approximately 10,000 m^2. Figure 5 shows the layout of the dynamic compaction patterns and the in situ test locations. The square symbol represents the locations of the first stage tamping, and the diamond symbol represents the locations of the second stage tamping. The smaller square area (440 m^2), shown at the lower right corner of Fig. 5, is a pilot (trial) test area. The capacity of equipment is 1200 kN (120 tons). The weight of tamper is 250 kN (25 tons) and the drop height is 20 m. The bottom area of the tamper is 3 m^2. In each stage, the number of drops is selected at 10 based on the trial tamping for effectiveness, and the grid spacing is 5 m. In this pilot test, it is necessary to confirm the depth of improvement. The depth improvement is defined as the maximum depth to which dynamic compaction caused improvement in a given soil property (*i.e.* penetration resistance). The depth improvement is a function of the drop energy, it can be expressed as

$$D = n\sqrt{WH} \tag{1}$$

where D = depth of improvement in meters; W = tamper weight in tons; H = drop height in meters; n is an empirical constant, n may vary between 0.3 ~ 0.8. Lukas (1995) suggested that 0.5 was a reasonable first approximation for n value. Figure 6 was shown

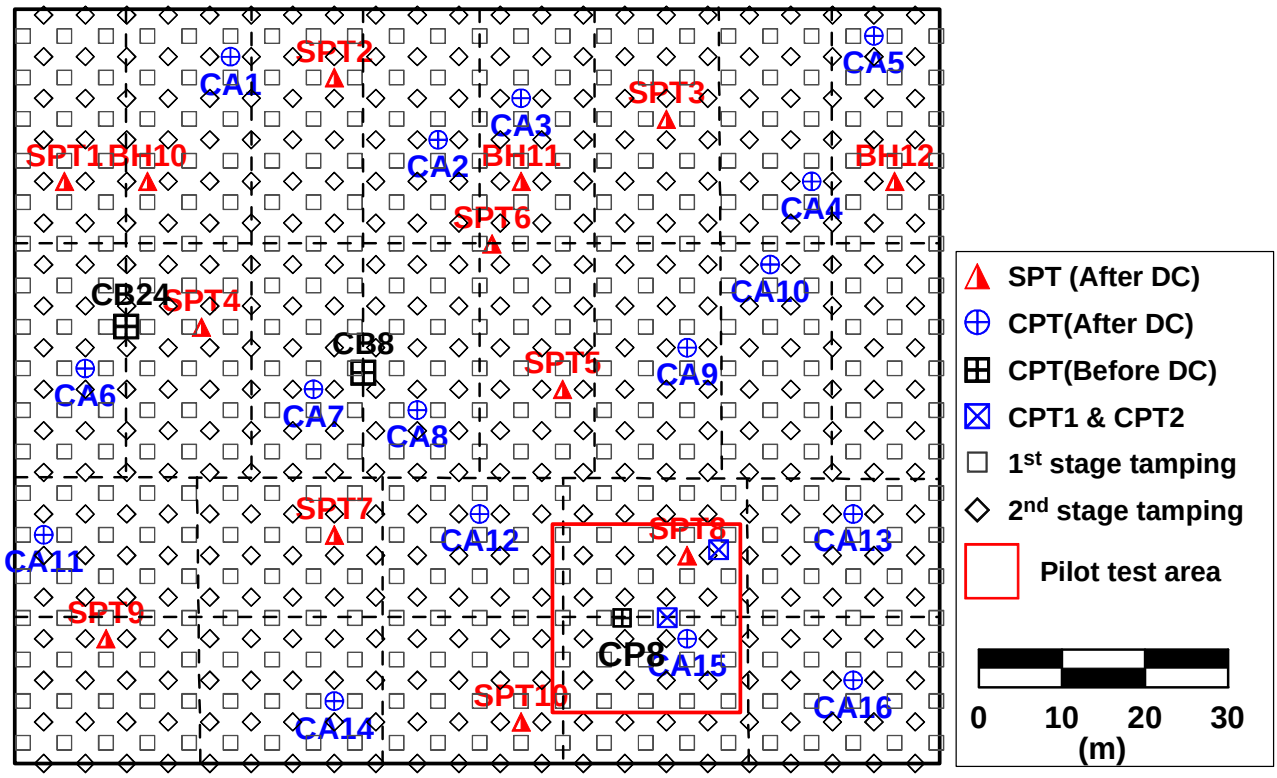

Fig. 5 Dynamic compaction patterns with layout of field tests and pilot test area

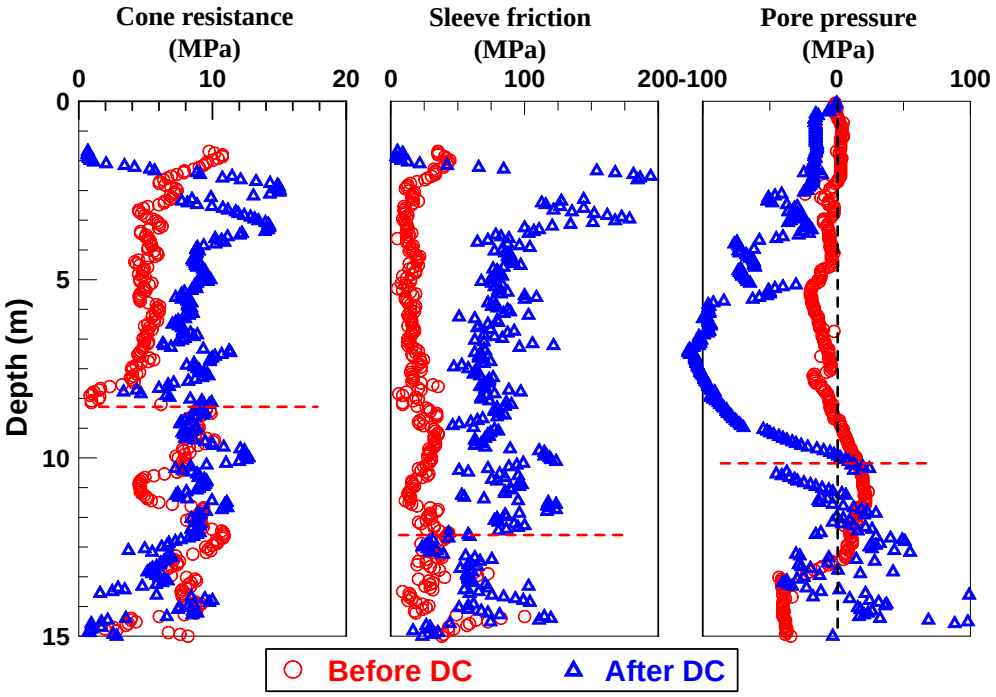

Fig. 6 Change in the CPT profiles before and after dynamic compaction in pilot test area

the change of CPT profile before and after dynamic compaction in the pilot test area. According to the cone resistance (q_c), sleeve friction (f_s), and the pore pressure (u_2) profiles the maximum depth of improvement was about 8.5 m, 12.1 m, and 10.2 m respectively.

The results of the pilot test confirmed the loose soil layer successfully compacted by taking those variables into consideration.

It should be noted that dynamic compaction has been widely employed in geotechnical engineering practice. The effectiveness of dynamic compaction for ground densification depends on several factors, such as the type of soils, the depth to the groundwater table, and the tamping pattern and parameters (grid dimensions, number of passes, weight of tamper, height of drop, number of drops, *etc*.). The design of the tamping pattern and parameters is usually carried out with empirical methods and guided by the results of the trial (pilot) tamping program and field monitoring. In this regard, it is noted that a considerable amount of experience and knowledge have been generated from past studies (Menard and Broise 1975; Mayne *et al*. 1984; Lukas 1995; Pasdarpour *et al*. 2009). In the present study, the focus is to examine the effect of dynamic compaction on the cone penetration sounding characteristics and liquefaction hazards (in depth 2 m ~ 10 m). The reader is referred to the aforementioned references on the subject of dynamic compaction.

4. CONE PENETRATION SOUNDING CHARACTERISTICS BEFORE AND AFTER DYNAMIC COMPACTION

Twelve of the 15 zones of the site that was subjected to dynamic compaction had been investigated with CPTu soundings before the ground improvement work. These prior CPTu soundings along with the post-compaction penetration soundings at near-by locations in these zones provide a basis for an examination of the soil characteristics as altered by dynamic compaction. The variations in the soil characteristics as reflected by the changes in cone tip resistance (q_c), sleeve friction (f_s), and penetration porewater pressure (u_2), are summarized in the following.

Figure 7 shows the change of the q_c sounding profiles after dynamic compaction in this site, as reflected by 16 pairs of CPTu soundings. Within the planned depth of ground improvement (approximately 10 m), q_c values increase significantly, especially in depths of 2 m to 7 m. This result is consistent with the conclusion of Rollins and Kim (2010). They concluded that 80% of the total improvement occurs within the upper 60% of the improvement zone. It is noted that in some locations, there is virtually no increase in q_c at a depth of about 8 m. This is likely due to the existence of thin-layer of clayey material. Majdi *et al*. (2007) pointed out that cohesive sublayers have also a damping effect on the energy input. Rollins and Kim also found that clay layer in the profile appeared to absorb energy and severely reduced compaction effectiveness.

Figure 8 summarizes the average change in q_c across the entire site at various depths as a result of dynamic compaction. The increase in q_c generally becomes less significant as it goes deeper. One possible reason is that dynamic compaction is not as effective at this depth (8 m to 10 m) as in the shallower depth (2 m to 7 m). The other possible reason is that the original q_c values at this depth (8 m to 10 m) are already quite high ($q_c \approx 8$ MPa before dynamic compaction) and thus less improvement can be achieved.

Figure 9 shows the change of the f_s profiles after dynamic compaction. The results show the sleeve friction increases significantly as a result of dynamic compaction. The exception at the depth of 7 m to 8 m is likely due to the existence of thin-layer of clayey material. Figure 10 shows the average change in f_s across the entire site at various depths as a result of dynamic compaction. The trend of diminishing effect of dynamic compaction on the increase of f_s is similar to that observed for q_c shown previously in Fig. 8.

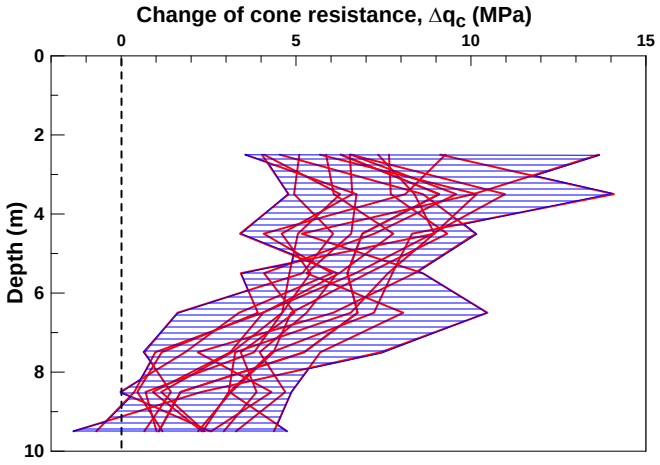

Fig. 7 Change in the q_c profiles after dynamic compaction

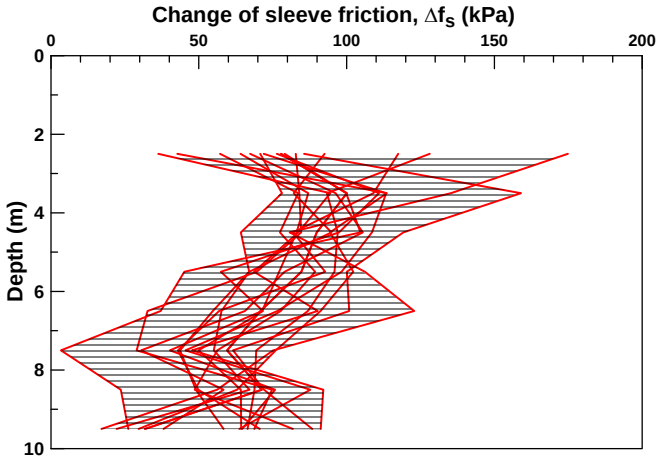

Fig. 9 Change in the f_s profiles after dynamic compaction

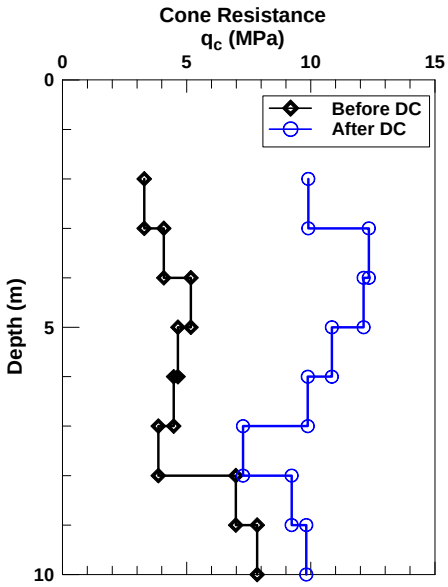

(a) q_c profiles before and after DC

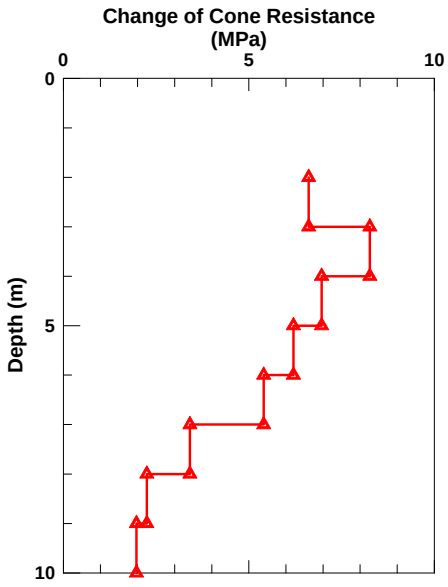

(b) Average change in q_c after DC

Fig. 8 Average change in q_c across the entire site at various depths

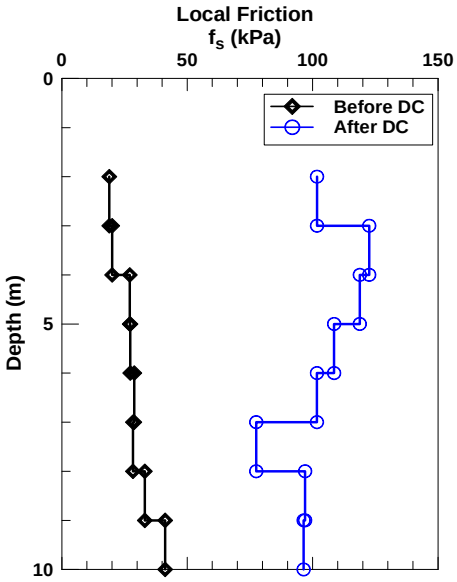

(a) f_s profiles before and after DC

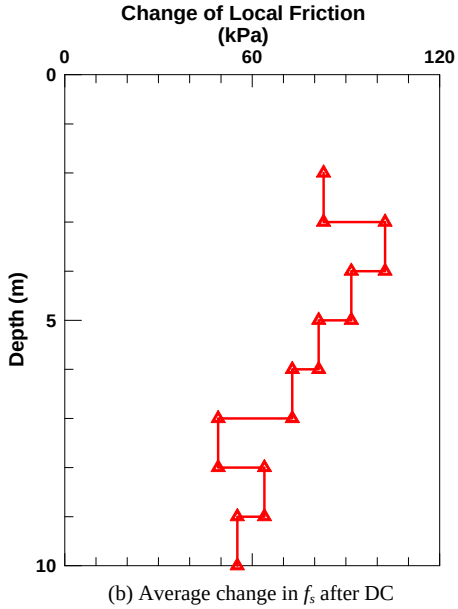

(b) Average change in f_s after DC

Fig. 10 Average change in f_s across the entire site at various depths

Generally, normally consolidated sandy soils represent approximately drained penetration. The penetration pore pressure is usually less than the hydrostatic water pressure. Very dense fine or silty sands can give very low or negative pore pressures. Soft to medium stiff clays can give small cone resistance and penetration pore pressure can be large, the penetration porewater pressure is usually greater than the hydrostatic water pressure. The change in the penetration porewater pressure after dynamic compaction offers another way to examine the effect of dynamic compaction. Figure 11 shows the changes in the penetration porewater pressure at the site. In general, the soils become denser as a result of dynamic compaction, which is reflected in greater negative penetration porewater pressure.

5. VARIATION IN SOIL BEHAVIOR TYPES

Cone penetration involves no sampling, and soil classification according to CPT is different from those carried out according to the Unified Soil Classification System (USCS); soil type determined with CPTu data is referred to as the soil behavior type (Robertson 1990). In theory, the dynamic compaction generates stress waves that densify the soils, and thus, soil type at depths will not be altered in the process (except at the point of contact where some change in particle size and distribution might be possible). However, the dynamic compaction can alter the values of q_c, f_s, and u_2, as discussed previously. Thus, it would be of interest to examine the possible variation of soil behavior type.

Figure 12 shows typical results (data points plotted on the soil behavior classification chart) from a selected location before and after dynamic compaction (soundings CB24 and CA6 in Fig. 5). Results from other locations reveal similar patterns and are not shown herein. Although the data points have "shifted" from looser state into denser state (mostly become overconsolidated sands as shown in the classification chart), the soil behavior type remains almost unchanged. Before the dynamic compaction, the soils are mostly in the range of type 6 (sands: Clean sand to silty sand) to type 5 (sand mixture: Silty sand to sandy silt). After the compaction, the classification largely remains the same, although the soils become denser.

Another way to examine this change is to compare the profile of soil behavior type index (I_c) before and after the compaction. Figure 13 shows such a comparison at all locations. Although some changes in the numerical values of I_c are observed (see also Fig. 14 for the magnitude of these changes on the average across the entire site), the soil behavior types largely remain the same.

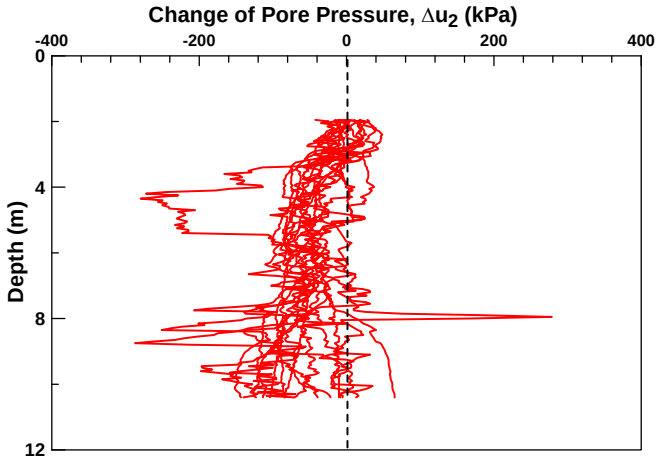

Fig. 11 Changes in the penetration pore pressure profiles after dynamic compaction

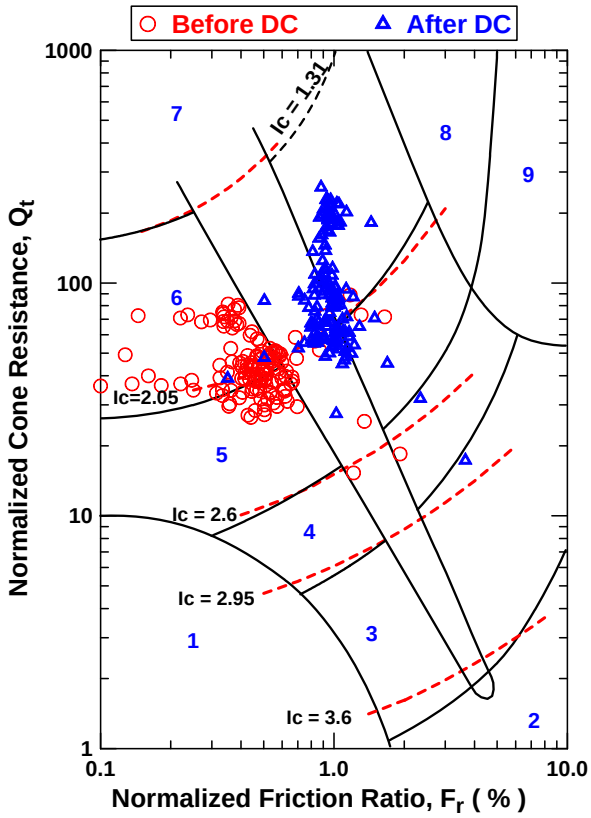

Fig. 12 Soil behavioral classification before and after dynamic compaction in zone Z17

6. VARIATION IN LIQUEFACTION POTENTIAL AND LIQUEFACTION-INDUCED SETTLEMENT

A common practice to investigate the effectiveness of dynamic compaction in reducing the risk of liquefaction is to compute factor of safety (F_S) against the initiation of liquefaction. In this regard, the SPT-, CPT-, or shear wave velocity (Vs)-based simplified methods, as summarized in Youd *et al*. 2001, can be used to compute the safety factor at a given depth. The scope of this paper is limited to use of CPT. Because CPT soundings provide practically continuous profiles of soil resistance, the profiles of safety factor, denoted as the F_S profiles, can be prepared before and after the compaction for a design seismic shaking level (for example, Majdi *et al*. 2007). While such profiles are useful in providing a graphical and qualitative comparison of liquefaction risk, many investigators prefer the use of liquefaction potential index (LPI) as a measure of liquefaction risk. The concept of LPI was first introduced and calibrated by Iwasaki *et al*. (1978, 1982). It considers the thickness of liquefied layer, the depth to the liquefied layer, and the liquefaction potential (in terms of safety factor) of the layer in its formulation; the concept is simple and logical, which yields an index for liquefaction risk at a site (represented by a soil profile). The index LPI is defined as follows:

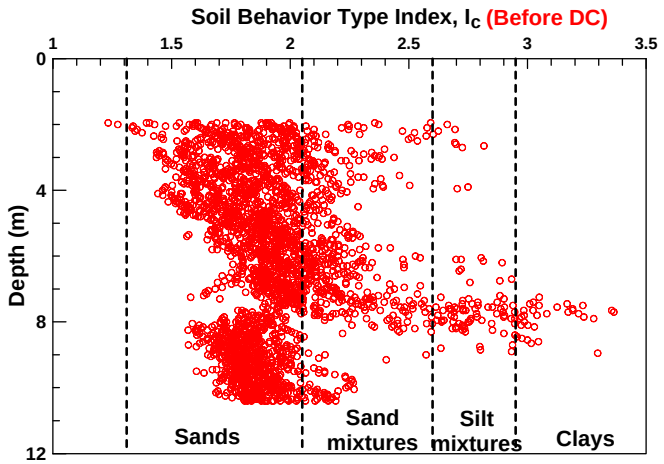

(a) I_c profiles before DC

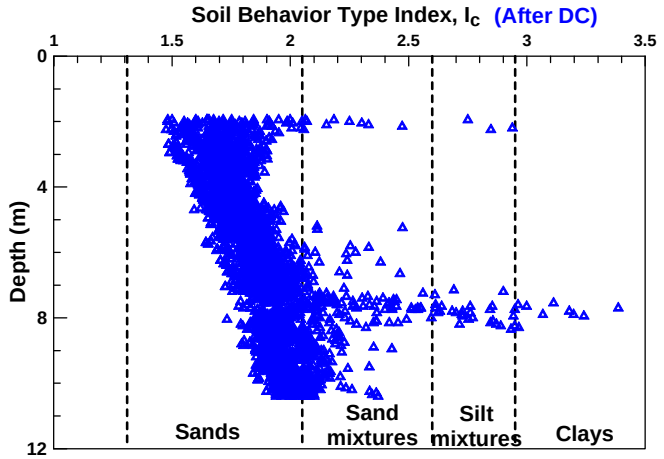

(b) I_c profiles after DC

Fig. 13 The I_c profiles before and after dynamic compaction

$$LPI = \sum_{0}^{20} F_l \times W(z)\, dz \tag{2}$$

where F_l is an index defined as: $F_l = 1 - Fs$, if $Fs \le 1.0$; and $F_1 = 0$ if $Fs > 1.0$. $W(z)$ is a weight function of the depth, which is used to estimate the contribution of soil liquefaction at different depth to the failure of the ground. The weight function is assumed to be a linear function:

$$W(z) = 10 - 0.5\, z \tag{3}$$

Many investigators have contributed to the calibration of LPI (Luna and Frost 1998; Sonmez 2003; Lee *et al*. 2003; Sonmez and Gokceoglu 2005; Li *et al*. 2006; Papathanassiou 2008; Juang *et al*. 2008). Although any of these methods can be used for the analysis of liquefaction risk before and after the dynamic compaction, the procedure and calibration results reported by Lee *et al*. (2003) is followed herein because it was conducted in the same general area as in the present study. In the study by Lee *et al*. (2003), the factor of safety was computed using the CPT-based method proposed by Robertson and Wride (1998), and the LPI was computed with the original formulation by Iwasaki *et al*. (1982). For the silty fine sands in the study area, the limits for low and high risk of liquefaction were determined to be 13 and 21, respectively, by Lee *et al*. (2003).

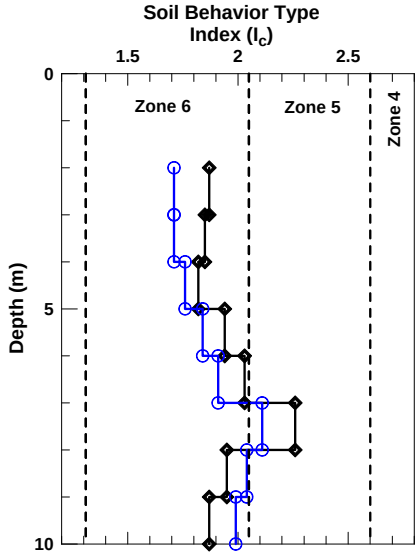

(a) I_c profiles before and after DC

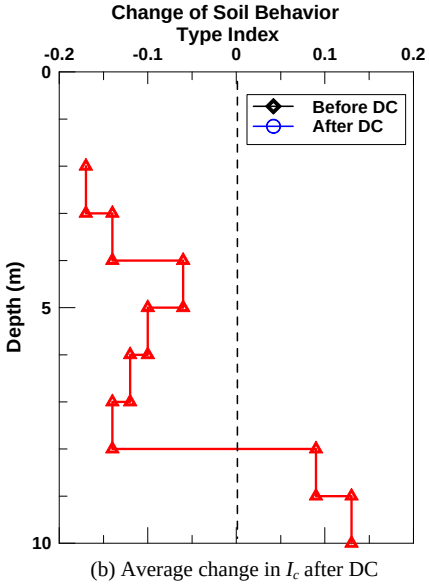

(b) Average change in I_c after DC

Fig. 14 Average change in I_c across the entire site at various depths

Figure 15 shows the computed LPI values using each of the 16 CPTu soundings from the 12 zones before and after the dynamic compaction. For this analysis, the groundwater table is assumed at a depth of 2.5 m, and the moment magnitude (M_w) is assumed to be 7.5; the analysis is carried out for different peak horizontal ground accelerations (a_{max}). The range of ground shaking levels reflected in this analysis is considered comparable to the 1999 Chi-Chi, Taiwan earthquake. The results show that before dynamic compaction, the site generally has a high to extremely high liquefaction risk; in fact, when a_{max} reaches 230 gal, the computed LPI values almost indicate a extremely high risk. On the other hand, this figure also shows the results after the dynamic compaction, indicating much lower risks. At a_{max} = 230 gal, all CPTu sounding locations indicate a low risk. The results are consistent with the observations in the same general coastal area with similar geological conditions in the 1999 Chi-Chi earthquake, as reported by Lee *et al*. (2001). Without ground improvement, the coastal reclaimed lands that were created by hydraulic filling are very susceptible to liquefaction risk; with properly conducted ground improvement by dynamic compaction, this liquefaction risk can be greatly reduced.

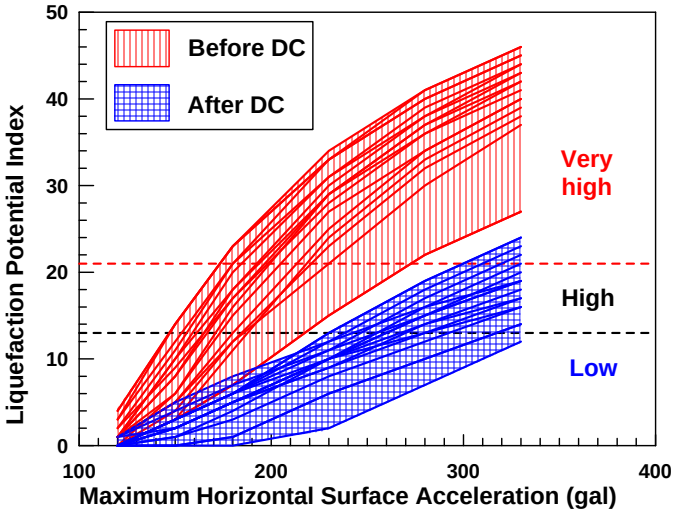

Fig. 15 Liquefaction potential index values before and after dynamic compaction

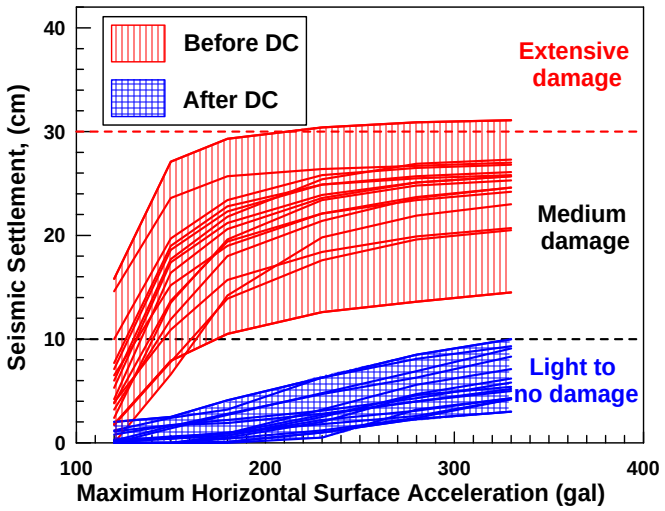

Fig. 16 Liquefaction-induced settlement before and after dynamic compaction

Another way to examine the liquefaction hazards is to compute possible settlements induced by liquefaction. Many investigators have contributed to this subject (for example, Tokimatsu and Seed 1984; Ishihara and Yoshimine 1992; Shamoto *et al*. 1998; Zhang *et al*. 2002; Tsukamoto *et al*. 2004; Cetin *et al*. 2009). In this paper, the CPT-based procedure proposed by Zhang *et al*. (2002) is adopted for the analysis of liquefaction-induced settlement. Based on the field observations, Ishihara and Yoshimine (1992) rated the ground damage as "Light to no damage" if the settlement is less than 10 cm, "Medium damage" if the settlement is between 10 cm and 30 cm, and "Extensive damage" if the settlement is greater than 30 cm. Figure 16 shows the results of the settlement analysis for the site before and after the dynamic compaction. The ground shaking conditions are the same as in the previous analysis for the LPI. At the a_{max} = 180 gal shaking level, the computed settlements all indicate a "Medium damage." This figure also shows the results of the analysis for the site after the dynamic compaction. These settlement results all indicate a "Low to no damage" even if a_{max} is 330 gal.

The results of the previous liquefaction potential and settlement analysis are consistent with field observations in the 1995 Hyogoken-Nambu earthquake. Ishihara and Cubrinovski (2005) reported that fewer signs of liquefaction were found in reclaimed deposits that had been treated by ground improvement measures; only scattered sand boils and smaller settlement of the ground were observed in the areas of compacted fill deposits. Majdi *et al*. (2007) shown the liquefaction potential was successfully mitigated by the dynamic compaction method for the nine oil tanks at the CROS project site.

7. CONCLUDING REMARKS

A case study of the effectiveness of dynamic compaction as a means for reducing the liquefaction hazards at a reclaimed land created by hydraulic filling is presented. Emphasis of the paper, however, is placed on examining the effect of dynamic compaction on the changes in the piezocone penetration sounding characteristics of the hydraulic-filled site and the resulting alteration of the liquefaction risk. The results show that dynamic compaction can increase the cone tip resistance (q_c) and sleeve friction (f_s) of soils in the expected depth of improvement (roughly from 2 m to 10 m). The quantity of the increase in q_c and f_s decreases with the increase of the depth. However, at some depths where thin-layer of clayey soils is, there is virtually no change in q_c and f_s. Furthermore, the change in the penetration porewater pressure (u_2) also signals the densification by dynamic compaction. As the sands become more over-consolidated after the dynamic compaction, the magnitude of the negative penetration porewater pressure (u_2) becomes greater.

While significant changes in q_c, f_s, and u_2 are observed after the dynamic compaction, the soil behavior type largely remains unchanged. The average changes in the soil behavior type index (I_c) are within the range of –0.2 to 0.2 across the entire site. When the data are plotted on the classification chart, those after DC data point locations appear to have shifted toward the direction of over-consolidated soils. However, the soil behavior types of these data remain largely unchanged after the dynamic compaction. This is consistent with the observation of the changes in the penetration porewater pressure.

Finally, the changes in liquefaction resistance after the dynamic compaction are observed. The well-accepted method by Robertson and Wride (1998) are used for evaluating the liquefaction resistance. In this method, the liquefaction resistance is a function of the normalized cone tip resistance (which is mainly affected by q_c) and the soil behavior type index I_c. Although the dynamic compaction does not change much on soil type (and I_c), it did increase q_c significantly, and as a result, the liquefaction resistance is increased significantly for the predominately silty sands (within the depth of ground improvement) at this site. Thus, in terms of the two measures of liquefaction hazards, the liquefaction potential index and the liquefaction-induced settlement, the risk is significantly reduced by the dynamic compaction.

ACKNOWLEDGEMENTS

The CPTu sounding profiles were obtained from several projects at the site, primarily conducted by the Rock Mechanics

Laboratory of the Department of Civil Engineering, National Cheng Kung University, Taiwan. Permission to use these CPTu data was granted by Dr. Der-Her Lee. The first author wishes to acknowledge the support of the National Science Council of Taiwan, which makes it possible for him to conduct research at Clemson University where the bulk of work was completed.

REFERENCES

Cetin, K. O., Bilge, H. T., Wu, J., Kammerer, A., and Seed, R. B. (2009). "Probabilistic models for the assessment of cyclically-induced reconsolidation (volumetric) settlements." *Journal of Geotechnical and Geoenvironmental Engineering*, **135**(3), 387–398.

Chang, C. T, Tseng, W. D., and Hsu, C. Y. (2002). "Ground improvement of coastal industrial parks in Taiwan." *Sino Geotechnics*, **93**, 53–68.

Ishihara, K. and Cubrinovski, M. (2005). "Characteristics of ground motion in liquefied deposits during earthquakes." *Journal of Earthquake Engineering*, **9** (Special Issue 1), 1–15.

Ishihara, K. and Yoshimine, M. (1992). "Evaluation of settlements in sand deposits following liquefaction during earthquakes." *Soils and Foundations*, **32**(1), 173–188.

Iwasaki, T., Tatsuoka, F., Tokida, K., and Yasuda, S. (1978). "A practical method for assessing soil liquefaction potential based on case studies at various sites in Japan." *Proceedings of the 2nd International Conference on Microzonation*, San Francisco, 885–896.

Iwasaki, T., Arakawa, T., and Tokida, K. (1982). "Simplified procedures for assessing soil liquefaction during earthquakes." *Proceedings of the Conference on Soil Dynamics and Earthquake Engineering*, Southampton UK, 925–939.

Juang, C. H., Liu, C. N., Chen, C. H., Hwang, J. H., and Lu, C. C. (2008). "Calibration of liquefaction potential index: A re-visit focusing on a new CPTU model." *Engineering Geology*, **102**(1/2), 19–30.

Lee, D. H., Juang, C. H., and Ku, C. S. (1999). "Liquefaction performance of soils at the site of a partially completed ground improvement project during the 1999 Chi-Chi earthquake in Taiwan." *Canadian Geotechnical Journal*, **38**(6), 1241–1253.

Lee, D. H., Ku, C. S., and Yuan, H. (2003). "A study of the liquefaction risk potential at Yuanlin, Taiwan." *Engineering Geology*, **71**(1/2), 97–117.

Leonards, G. A., Cutter, W. A., and Holtz, R. D. (1980). "Dynamic compaction of granular soils." *Journal of Geotechnical Engineering*, ASCE, **106**(GT1), 35–44.

Li, D. K., Juang, C. H., and Andrus, R. D. (2006). "Liquefaction potential index: A critical assessment." *Journal of GeoEngineering*, **1**(1), 11–24.

Lukas, R. T. (1995) Dynamic compaction. Geotechnical Engineering Circular No. 1, Publication no. FHWA-SA-95-037.

Luna, R. and Frost, J. D. (1998). "Spatial liquefaction analysis system." *Journal of Computing in Civil Engineering*, **12**(1), 48–56.

Majdi, A., Soltani, A. S., and Litkouhi, S. (2007). "Mitigation of liquefaction hazard by dynamic compaction." *Ground Improvement*, **11**(3), 137–143.

Mayne, P. W., Jones, J. S., and Dumas, J. C. (1984). "Ground response to dynamic compaction." *Journal of Geotechnical Engineering*, ASCE, **110**(JT6), 757–773.

Massarsch, K. R. and Fellenius, B. H. (2002). "Vibratory compaction of coarse-grained soils." *Canadian Geotechnical Journal*, **39**(3), 695–709.

Menard, L. and Broise, Y. (1975). "Theoretical and practical aspects of dynamic consolidation." *Geotechnique*, **25**(1), 3–18.

Pan, J. and Hwang, Z. M. (1995). "Soil densification by dynamic consolidation for Formosa heavy industries corp." *Sino Geotechnics*, **51**, 35–50.

Papathanassiou, G. (2008). "LPI-based approach for calibrating the severity of liquefaction-induced failures and for assessing the probability of liquefaction surface evidence." *Engineering Geology*, **96**(1/2), 94–104.

Pasdarpour, M., Ghazavi, M., Teshnehlab, M., and Sadrnejad, S. A. (2009). "Optimal design of soil dynamic compaction using genetic algorithm and fuzzy system." *Soil Dynamics and Earthquake Engineering*, **29**(7), 1103–1112.

Robertson, P. K. and Wride, C. E. (1998). "Evaluating cyclic liquefaction potential using the cone penetration test." *Canadian Geotechnical Journal*, **35**(3), 442–459.

Robertson, P. K. (1990). "Soil classification using the cone penetration test." *Canadian Geotechnical Journal*, **27**(1), 151–158.

Rollins, K. M. and Kim, J. (2010). "Dynamic compaction of collapsible soils based on U.S. case histories." *Journal of Geotechnical and Geoenvironmental Engineering*, **136**(9), 1178–1186.

Shamoto, Y., Zhang, J. M., and Tokimatsu, K. (1998). "Methods for evaluating residual post-liquefaction ground settlement and horizontal displacement." *Special Issue on the Geotechnical Aspects of the January*, 17 1995 Hyogoken-Nambu Earthquake, 69–83.

Sonmez, H. (2003). "Modification of the liquefaction potential index and liquefaction susceptibility mapping for a liquefaction-prone area." *Environmental Geology*, **4**(7), 862–871.

Sonmez, H. and Gokceoglu, C. (2005). "A liquefaction severity index suggested for engineering practice." *Environmental Geology*, **48**(1), 81–91.

Tokimatsu, K. and Seed, H. B. (1984). "Simplified procedures of the evaluation of settlements in clean sands." *Report No. UCB/GT-84/16*, University of California, Berkeley, California.

Tsukamoto, Y., Ishihara, K., and Sawada, S. (2004). "Settlement of silty sand deposits following liquefaction during earthquakes." *Soils and Foundations*, **44**(5), 135–148.

Youd, T. L., Idriss, I. M., Andrus, R. D., Arango, I., Castro, G., Christian, J. T., Dobry, R., Liam Finn, W. D., Harder, L. F., Jr Hynes M. E., Ishihara, K., Koester, J. P., Laio, S. S. C., Marcuson, W. F. III, Martin, G. R., Mitchell, J. K., Moriwaki, Y., Power, M. S., Robertson, P. K., Seed, R. B., and Stokoe, K. H. II. (2001). "Liquefaction resistance of soils: Summary report from the 1996 NCEER and 1998 NCEER/NSF workshops on evaluation of liquefaction resistance of soils." *Journal of Geotechnical and Geoenvironmental Engineering*, **127**(10), 817–833.

Yu, M. S., Shieh, B. C., and Chung, Y. T. (2000). "Liquefaction induced by Chi-Chi Earthquake on reclaimed land in central Taiwan." *Sino-Geotechnics*, **77**, 39–50.

Zhang, G., Robertson, P. K., and Brachman, R. W. I. (2002). "Estimating liquefaction-induced ground settlements from CPT for level ground." *Canadian Geotechnical Journal*, **39**(5), 1168–1180.